

## $L = 1$ Excitation in the Halo Nucleus $^{11}\text{Li}$

A. A. Korshennikov,<sup>1,\*</sup> E. A. Kuzmin,<sup>2</sup> E. Yu. Nikolskii,<sup>2</sup> O. V. Bochkarev,<sup>2</sup> S. Fukuda,<sup>1</sup> S. A. Goncharov,<sup>3</sup> S. Ito,<sup>1</sup>  
T. Kobayashi,<sup>1</sup> S. Momota,<sup>1</sup> B. G. Novatskii,<sup>2</sup> A. A. Ogloblin,<sup>2</sup> A. Ozawa,<sup>1</sup> V. Pribora,<sup>2</sup> I. Tanihata,<sup>1</sup> and K. Yoshida<sup>1</sup>

<sup>1</sup>RIKEN, 2-1 Hirosawa, Wako, Saitama, 351-01, Japan

<sup>2</sup>The Kurchatov Institute, Kurchatov sq. 1, Moscow 123182, Russia

<sup>3</sup>Institute of Nuclear Physics, Moscow State University, Moscow 119899, Russia

(Received 5 November 1996)

Collisions of  $^{11}\text{Li} + p$  at 68A MeV have been studied by correlational measurements. An excited state of  $^{11}\text{Li}$  at  $E^* \approx 1.3$  MeV was observed. The measured angular distributions show the dipole nature of the excitation of the 1.3-MeV peak. The structure of the excited states and the ground state of  $^{11}\text{Li}$  is discussed. [S0031-9007(97)02800-7]

PACS numbers: 25.60.-t, 21.10.Re, 23.20.En, 27.20.+n

The  $^{11}\text{Li}$  nucleus presents one of the most widely known and exciting problems in modern nuclear physics. Numerous experimental and theoretical studies of  $^{11}\text{Li}$  were performed after the discovery of an extraordinary large radius of  $^{11}\text{Li}$  [1], which reflects such a fascinating and hitherto unknown phenomenon as a neutron halo [2]: The spatial extension of two valence neutrons beyond the  $^9\text{Li}$  core to distances larger than the range of nuclear forces and into a region, which is forbidden in classical physics. A very interesting question arises about the type of motion in such an exotic system corresponding to an excitation of the neutron halo. As a consequence of the existence of a halo, a unique phenomenon, the soft dipole mode of excitation, was suggested [3], which makes corresponding experimental studies especially intriguing. Such experiments are also stimulated by the fact that the mechanism of the halo excitation is strongly related to the structure of the ground state of  $^{11}\text{Li}$ , which is not yet well understood. For instance, the question regarding the orbital momenta of the valence neutrons has not yet been answered and it is under intensive investigation, both experimentally and theoretically.

In Ref. [4] we reported an observation of the  $^{11}\text{Li}$  excited state at  $E^* \approx 1.25$  MeV, which is considered to be the halo excitation. The experimental result of Ref. [4] agrees with the first hint on the  $^{11}\text{Li}$  low-lying state obtained in the reaction  $^{11}\text{B}(\pi^-, \pi^+)^{11}\text{Li}$  [5], and it was recently also confirmed by the invariant mass measurements of  $^9\text{Li} + n + n$  from fragmentation of  $^{11}\text{Li}$  on a carbon target [6].

In this paper we present a new spectroscopic study of  $^{11}\text{Li}$  by scattering of  $^{11}\text{Li} + p$ . The key features of the experiment were the use of a radioactive beam and correlational measurement of emitted particles. We succeeded in measuring the angular distribution for the 1.3-MeV peak in  $^{11}\text{Li}$ . This angular distribution shows an  $L = 1$  transition character, and such a dipole nature of excitation in the neutron-rich halo nucleus  $^{11}\text{Li}$  runs contrary to the systematics for usual nuclei.

In the experiment we use a binary radioactive beam, which consisted of  $^{11}\text{Li}$  and  $^{14}\text{Be}$ , and simultaneously studied  $^{11}\text{Li} + p$  and  $^{14}\text{Be} + p$  collisions under inverse kinematical conditions. Results obtained for the neutron-halo nucleus  $^{14}\text{Be}$  will be published in another paper. The secondary beams were produced by the fragment separator RIPS (RIKEN, Japan) from fragmentation of the  $^{18}\text{O}$  primary beam at  $E = 100A$  MeV. The  $^{11}\text{Li}$  beam had energy  $E^{\text{lab}} = 68.4A$  MeV with an energy spread  $\Delta = \pm 3.5A$  MeV. The energy of the  $^{14}\text{Be}$  beam was  $E^{\text{lab}} = 73.6A$  MeV ( $\Delta = \pm 3.5A$  MeV). The RIPS was tuned to optimize  $^{14}\text{Be}$  intensity because this beam is weaker. The intensities of  $^{14}\text{Be}$  and  $^{11}\text{Li}$  were 3000 pps and 12 000 pps, respectively.

The experimental setup (Fig. 1) was similar to that used in our previous experiment in Ref. [4]. Applying the event-by-event method, we identified each projectile and measured its energy and trajectory using two plastic scintillators and MWPC's. The secondary beam hit  $\text{CH}_2$  and C targets with thicknesses of 48 and 48.6 mg/cm<sup>2</sup>, respectively. All experimental distributions presented in this paper correspond to a pure proton target (the negligible background from the C target was subtracted).

Applying the missing mass method, we detected recoil protons by two telescopes of solid state detectors with large areas. The centers of the telescopes were located at the laboratory angle of 70°, i.e., in the range of relatively small center-of-mass scattering angles. The telescopes measured the energy and angular coordinates of each proton, thereby

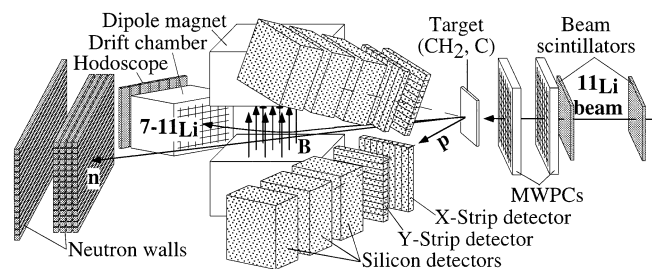


FIG. 1. The experimental setup.

allowing a determination of the excitation energy in the residual  $^{11}\text{Li}$ -like system. Resolution in the excitation energy of  $^{11}\text{Li}$  (FWHM = 2.2 MeV) was mainly due to the target thickness and the angular resolution of the setup. In the first measurement in Ref. [4] the resolution was better (FWHM = 1.5 MeV) due to the thinner target. In the present experiment we used a thicker target to compensate weaker secondary beams.

In addition to the recoil protons, we detected other particles emitted at forward angles. Charged particles (e.g., elastically scattered  $^{11}\text{Li}$  or  $^{9,8,7}\text{Li}$  from breakup of the projectile) were bent in the dipole magnet and measured by the drift chamber and the plastic scintillators' hodoscope. The hodoscope allowed determination of the charge of the detected particle, while the drift chamber was used for isotope identification. Neutrons from decay of  $^{11}\text{Li}$  were detected by layers of plastic scintillators. This part of the detection system allowed us to study exclusive spectra of protons detected in coincidences with particles from the projectile breakup. In the present experiment, unlike previous measurement in Ref. [4], there was full acceptance for these breakup particles. This has allowed us to obtain a reliable angular distribution for the 1.3-MeV peak in  $^{11}\text{Li}$ .

The resulting proton spectra presented in Fig. 2 as a function of the  $^{11}\text{Li}$  excitation energy correspond to the overall acceptance of the proton telescopes ( $\theta_p^{\text{lab}} \approx 60^\circ\text{--}80^\circ$ ). In Fig. 2(a), the solid histogram shows the inclusive spectrum of protons. A strong peak is seen from the  $^{11}\text{Li}$  ground state. The dotted histogram, which presents the spectrum of protons detected in coincidence  $p + ^{11}\text{Li}$ , corresponds to pure elastic scattering. It is seen that the left half of the dotted histogram coincides with the left side of the peak in the solid histogram, while on the right side the solid histogram exceeds the dotted one. It reflects the presence of the  $^{11}\text{Li}$  peak at  $E^* \approx 1.3$  MeV. This peak is clearly seen in Figs. 2(b)–2(d), where we present proton spectra detected in coincidences with particles from breakup of  $^{11}\text{Li}$ . Such coincidences exclude the strong elastic-scattering peak and select nonelastic scattering events only. Figures 2(b)–2(d) show proton spectra detected in  $p + ^{9,8,7}\text{Li}$ ,  $p + n$ , and  $p + n + ^{9,8,7}\text{Li}$  coincidence, respectively (for coincidences with Li isotopes, the  $^9\text{Li} + p$  events are predominant). The obtained parameters of the peak are  $E^* = 1.3 \pm 0.1$  MeV,  $\Gamma = 0.75 \pm 0.6$  MeV; they are in agreement with the previous measurement in Ref. [4]. Other states mentioned in Ref. [4] might not be seen because of insufficient resolution and lower yields than that for the 1.3-MeV peak.

Curves in Fig. 2(a) show typical physical backgrounds. They are smooth and clarify general trends in the high energy part of the spectrum. Curve 1 corresponds to phase space in the exit channel  $p + n + n + ^9\text{Li}$ . Curve 2 shows the result of calculations for the  $n + n$  final state interaction. Calculations for the  $n + ^9\text{Li}$  final state inter-

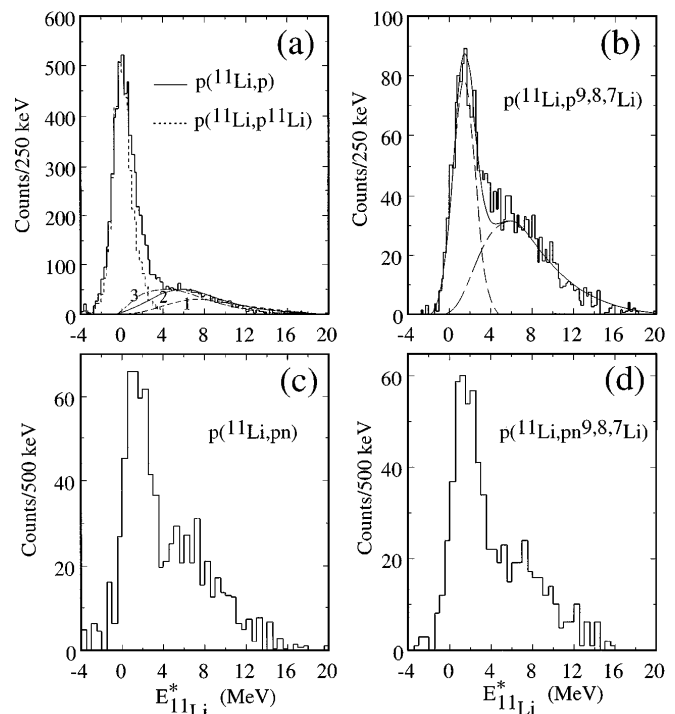


FIG. 2. Proton spectra as a function of the  $^{11}\text{Li}$  excitation energy. (a) The inclusive spectrum of protons (solid histogram) and the spectrum of protons detected in coincidence with  $^{11}\text{Li}$  (dotted histogram); curves present typical physical backgrounds: 1—phase space  $p + n + n + ^9\text{Li}$ ; 2—final state interaction  $n + n$  or  $n + ^9\text{Li}$  via a virtual state; 3—final state interaction  $n + ^9\text{Li}$  via a narrow resonance  $^{10}\text{Li}$ . (b) The proton spectrum detected in coincidence with  $^{9,8,7}\text{Li}$ ; the solid curve shows a fit of the spectrum with a Gaussian (the dashed curve) and the dash-dotted curve calculated for the final state interaction via a virtual state. (c) The proton spectrum detected in coincidence with neutron. (d) The proton spectrum in triple coincidence  $p + n + ^{9,8,7}\text{Li}$ .

action, via a virtual state with parameters giving a low energy peak in the system  $^{10}\text{Li}$  [7,8], give results practically identical to curve 2. Curve 3 corresponds to the  $n + ^9\text{Li}$  final state interaction in the state  $^{10}\text{Li}$ , which was considered as a low energy resonance with negligible width. In the calculations, detection acceptances and resolutions were taken into account. The curves in Fig. 2(b) show an example of fit of the spectrum with a Gaussian for the 1.3-MeV peak (dashed curve) and with the curve calculated for the final state interaction via the virtual states  $n + n$  or  $n + ^9\text{Li}$  (dash-dotted curve).

Angular distributions for the elastic scattering  $^{11}\text{Li}(p, p)^{11}\text{Li}$  and for excitation of the  $^{11}\text{Li}$  peak at  $E^* \approx 1.3$  MeV are presented in Fig. 3. The inelastic scattering angular distribution in Fig. 3 was extracted from  $p + ^{9,8,7}\text{Li}$  coincidences. Use of the  $p + n + ^{9,8,7}\text{Li}$  coincidences yields a very similar distribution. In Fig. 3, errors for the inelastic scattering cross section include both statistical errors and uncertainties in subtraction of the pedestal under the peak in the proton

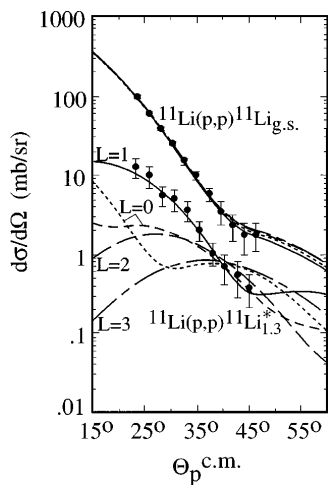


FIG. 3. Angular distributions for the elastic and inelastic scattering of  $^{11}\text{Li} + p$  at 68A MeV. Curves show the results of coupled channel calculations for the  $^{11}\text{Li}$  excitation with transferred orbital angular momentum  $L = 0, 1, 2, 3$ . For  $L = 0$ , the long-dashed curve shows the result of calculations with the breathing-mode form factor [11].

spectrum. The systematic error of the absolute value of the cross section is  $\sim 5\%$ .

The measured cross sections were analyzed in the following way. First, we fitted the elastic scattering angular distribution starting from the optical potential, found in Ref. [9] for the  $p + ^{11}\text{Li}$  elastic scattering at 62A MeV measured in Ref. [10]. This potential contains real and imaginary volume components, a surface imaginary term, and a spin-orbital part. After this, the fitted potential was used in the coupled channel calculations for the  $^{11}\text{Li}$  excitation with transferred orbital angular momentum  $L = 0, 1, 2, 3$ . For  $L = 0$ , both the conventional form factor  $\beta dV/dr$  and the breathing mode [11] were investigated. Calculations were performed by means of the codes ECIS [12] and CHUCK [13]. The results are shown in Fig. 3. We repeated the same procedure starting from the potentials (i) without the surface imaginary term, (ii) without the imaginary volume part (that is, with only surface term) as well as (iii) for the potential, which contains only volume real and imaginary components. Final results are similar to the curves presented in Fig. 3. Further microscopic analysis of the measured cross sections performed in Ref. [14] yields the same shapes of calculated angular distributions for  $L = 0, 1, 2, 3$ .

As seen in Fig. 3, the experimental inelastic-scattering cross section definitely corresponds to  $L = 1$ . It is also seen that the slope of the experiment distribution can not be reproduced by combination of contributions with  $L = 0, 2$ , and  $3$ . This means that even if the observed 1.3-MeV peak includes more than one unresolved level of  $^{11}\text{Li}$ , the main strength still corresponds to the  $L = 1$  excitation. (For example, three states with  $J^\pi = \frac{1}{2}^+, \frac{3}{2}^+$ , and  $\frac{5}{2}^+$

would be consistent with  $L = 1$ .) Note that although statistics were low in the study of the  $^{11}\text{B}(\pi^-, \pi^+)^{11}\text{Li}$  reaction in Ref. [5], the angular distribution also was consistent with  $L = 1$ .

Therefore, the results obtained show that  $^{11}\text{Li}$  has an excited state at  $E^* \approx 1.3$  MeV corresponding to a dipole type of excitation.

This  $L = 1$  excitation can correspond to the following structure of  $^{11}\text{Li}^*$ . Omitting, for simplicity, the intrinsic spin parity of the  $^9\text{Li}$  core in the system  $n + n + ^9\text{Li}$ , one can conclude that the  $L = 1$  transition from the ground state with  $J^\pi = 0^+$  can excite states produced by the following terms with lowest partial waves:

$$|l_{n-n} = S_{nn} = 0, l_{^9\text{Li}-nn} = 1, L = 1, J^\pi = 1^-\rangle, \quad (1)$$

$$|l_{n-n} = S_{nn} = 1, l_{^9\text{Li}-nn} = 0, L = 1, J^\pi = 0^-\rangle, \quad (2)$$

$$|l_{n-n} = S_{nn} = 1, l_{^9\text{Li}-nn} = 0, L = 1, J^\pi = 1^-\rangle, \quad (3)$$

$$|l_{n-n} = S_{nn} = 1, l_{^9\text{Li}-nn} = 0, L = 1, J^\pi = 2^-\rangle. \quad (4)$$

(Here  $l_{c-ab}$  is the orbital momentum between particle  $c$  and the center of mass of  $a$  and  $b$ ,  $S_{nn}$  is the total spin of two neutrons,  $\hat{L} = \hat{l}_{a-b} + \hat{l}_{ab-c}$ ,  $\hat{J} = \hat{L} + \hat{S}_{nn}$ ). The wave functions (1)–(4) are antisymmetrized relative to permutation of two valence neutrons. To study the role of the Pauli principle in the  $n + ^9\text{Li}$  subsystem, we transformed (1)–(4) to the coordinates, which contain orbital momentum between the neutron and  $^9\text{Li}$  and their total momentum, using Reinal-Revai coefficients and  $9J$  symbols. All four wave functions (1)–(4) are a mixture of  $s$  and  $p$  motion in the subsystem  $n + ^9\text{Li}$ . Terms (1), (3), and (4) necessarily contain an admixture of the  $p_{3/2}$  state in the  $n + ^9\text{Li}$  subsystem. Since the  $p_{3/2}$  neutron orbital is already occupied in  $^9\text{Li}$ , these terms are suppressed. The wave function (2) has no  $p_{3/2}$  admixture and contains only  $p_{1/2}$  (and  $s$ ) states. Thus, the excited state of  $^{11}\text{Li}$  is consistent with the configuration (2) with  $J^\pi = 0^-$ . It contains a triplet state of valence neutrons [in (2),  $S_{nn} = 1$ ]. Another possibility arises from the fact that there are two terms, (1) and (3), with  $J^\pi = 1^-$ . One can combine them with a ratio of norms  $\sim 0.4$  [term (3) is stronger] to compensate contribution of the  $p_{3/2}$  state in the  $n + ^9\text{Li}$  subsystem. The resultant wave function is also consistent with the observed peak in  $^{11}\text{Li}$ . Since the term (3) is stronger than (1), the total wave function again contains a strong component of  $S_{nn} = 1$  ( $\sim 70\%$ ).

Thus, both possible configurations of  $^{11}\text{Li}^*$  contain the triplet state of valence neutrons. To excite such a state starting from the  $^{11}\text{Li}$  ground state with  $S_{nn} = 0$  requires a spin-flip process. This process is known to have low cross section, while the observed cross section is large. To excite  $^{11}\text{Li}^*$  with large cross section by a one-step process is possible if the ground state also contains a component of valence neutrons in the triplet state (and the transition  $^{11}\text{Li}_{\text{g.s.}} \rightarrow ^{11}\text{Li}^*$  can be interpreted as changing of  $l_{^9\text{Li}-nn}$  by  $\Delta l = 1$ ). The  $S_{nn} = 1$  component in the

ground state is equivalent to valence neutrons in the  $p_{1/2}$  orbital, since such a  $p_{1/2}$  component of the  $n + n + {}^9\text{Li}$  wave function contains  $S_{nn} = 1$  with a large weight of  $\sim 70\%$ , as can be seen from the corresponding  $9J$  symbol.

Finally, the observed  $L = 1$  excitation is consistent with the  ${}^{11}\text{Li}$  excited state with  $J^\pi = 0^-$  and  $1^-$  (omitting the spin parity of  ${}^9\text{Li}$ ) and shows that the ground state of  ${}^{11}\text{Li}$  cannot have a structure with valence neutrons in pure  $s$  orbital, but must contain a significant component that has neutrons in the  $p_{1/2}$  orbital.

In summary, we have studied  ${}^{11}\text{Li} + p$  collisions at 68A MeV by correlational measurements. The experimental results show that  ${}^{11}\text{Li}$  has an excited state at  $E^* \simeq 1.3$  MeV with a dipole-type excitation. This state is consistent with quantum numbers in the  $n + n + {}^9\text{Li}$  system  $J^\pi = 0^-$  or  $1^-$  (omitting the spin parity of  ${}^9\text{Li}$ ). The observed  $L = 1$  excitation of  ${}^{11}\text{Li}$  shows that the ground state of  ${}^{11}\text{Li}$  cannot have a structure with valence neutrons in pure  $s$  orbital, but must contain a significant component of the  $p_{1/2}$  orbital.

\*On leave from the Kurchatov Institute, Moscow 123182, Russia.

- [1] I. Tanihata *et al.*, Phys. Rev. Lett. **55**, 2676 (1985).
- [2] P.G. Hansen and B. Jonson, Europhys. Lett. **4**, 409 (1987).
- [3] K. Ikeda, Nucl. Phys. **A538**, 355c (1992).
- [4] A.A. Korshennikov *et al.*, Phys. Rev. C **53**, R537 (1996).
- [5] T. Kobayashi, in Ref. [3], p. 343c.
- [6] M. Zinser *et al.* (to be published).
- [7] A.I. Amelin *et al.*, Sov. J. Nucl. Phys. **52**, 782 (1990).
- [8] R.A. Kryger *et al.*, Phys. Rev. C **47**, R2439 (1993).
- [9] S. Hirenzaki, H. Toki, and I. Tanihata, Nucl. Phys. **A552**, 57 (1993).
- [10] C.-B. Moon *et al.*, Phys. Lett. B **297**, 39 (1992).
- [11] G.R. Satchler, *Direct Nuclear Reactions* (Clarendon Press, Oxford, 1983), p. 588.
- [12] J. Reynal, Phys. Rev. C **23**, 2571 (1981).
- [13] P.D. Kunz, computer code CHUCK (unpublished).
- [14] R. Kanungo and C. Samanta, Nucl. Phys. A (to be published).